Geological Journal

WILEY

RESEARCH ARTICLE

Paleoenvironmental and Paleodepositional Reconstruction of the Permian Coals From Burhar Seam IV of Sohagpur Coalfield, India: Using Integrated Mineralogical, Geochemical and Petrographic Proxies

Kaushal Kishor[1] | Manish Kumar Srivastava[1] | Gyan Prakash Tripathi[1] | Alok K. Singh[1] | Soumyajit Mukherjee[2]

[1]Department of Petroleum Engineering and Geoengineering, Rajiv Gandhi Institute of Petroleum Technology, Amethi, Uttar Pradesh, India | [2]Department of Earth Sciences, Indian Institute of Technology Bombay, Mumbai, Maharashtra, India

Correspondence: Alok K. Singh (asingh@rgipt.ac.in)

Received: 1 July 2025 | **Revised:** 11 September 2025 | **Accepted:** 13 October 2025

Handling Editor: M. Ramkumar

Funding: The authors received no specific funding for this work.

Keywords: illite | kaolinite | maceral | Sharda coal mine | Sohagpur coalfield

ABSTRACT

Deciphering the paleoenvironment from coal samples is of great academic and industrial relevance. Coal samples from the Burhar seam IV, Sharda coalmine of the Sohagpur coalfield, were analysed using a multi-proxy approach to interpret paleoclimate and paleo-depositional conditions. The analysis incorporated several techniques, viz., Ultimate Analysis, X-ray Fluorescence (XRF), X-ray Diffraction (XRD), Fourier Transform Infrared (FT-IR) Spectroscopy and coal petrography. The Sohagpur coal deposit is a part of the Lower Gondwana coal group, which is characterised by high ash content resulting from proximate analysis. While XRD and FT-IR spectra identify the mineral components in the coal, XRF results show different oxide and elemental concentrations. Micropetrography provided insights into the maceral and mineral constituents of the samples. XRD, XRF and FT-IR results indicate a warm and humid paleoclimate favoured by intense chemical weathering, evidenced by the presence of minerals such as kaolinite. Depositional conditions were further examined through sulphur content analysis using Ultimate Analysis and elemental concentrations from the XRF. These suggest deposition in a transitional environment between oxic and suboxic conditions. Petrographic analysis also supported these findings, which indicate the coal samples were deposited in alternating oxic and anoxic moor conditions, with good tissue preservation.

1 | Introduction

Coal is used as a fossil fuel throughout the world. In India, especially, coal is not just an energy source but also a foundation for the country's social and economic development (Equeenuddin et al. 2016). India is the second-largest coal producer and stands fifth in the reserves worldwide (IBM 2021). The heterogeneity in coal comprises both organic and inorganic constituents, which are reflected by the physical, chemical, thermal and petrographic properties of the coal

Abbreviations: Ag, alginite; Arg, argillaceous mineral matter; ASTM, American Society for Testing and Materials; BET, Brunauer–Emmett–Teller; Bt, bituminite; Cb, carbonate mineral matter; Cd, collodetrinite; Cg, corpogelinite; Cl, collotelinite; Ct, cutinite; DV, dark vitrinite; Exd, exsudatinite; Fl, fluorinite; FT-IR, Fourier transform infrared; Fu, Fusinite; G, gelinite; I, inertinite; IBM, Indian Bureau of Mines; ICCP, International Committee for Coal and Organic Petrology; It, inertodetrinite; L, liptinite; Lt, litrodetrinite; Ma, macrinite; Mi, micrinite; MM, mineral matter; mmf, mineral matter free; P, pollen; PV, pseudo vitrinite; Py, pyrite; REEs, rare earth elements; Rs, resinite; Sb, suberinite; Se, secretinite; SEM-EDS, scanning electron microscopy–energy dispersive spectroscopy; Sf, semifusinite; Sp, sporinite; Tl-, telinite; V, vitrinite; Vt, vitrodetrinite; XRD, x-ray diffraction; XRF, x-ray fluorescence.

TABLE 1 | Several authors worked on different Indian terrains/basins on coal/lignite deposits, and their key findings are summarised in the table.

Sl No.	Author(s)	Terrain/coalfield/basin	Methodology used	Key finding	Proxies used organic/inorganic
1	Singh et al. (2003)	Deoghar basin	Petrographic characterisation of coal samples, analysis of macerals and micro-lithotypes	The Barakar coals evolved under comparatively wet moor conditions with intermittent moderate to high flooding.	Organic
2	Singh et al. (2012)	Tiru Valley	Petrography	Petrographic indices indicate the wet forest origin of these coals.	Organic
3	Singh (2016a)	Talcher coalfield, Mahanadi Basin	Petrography	The Tacher coals were formed in wet moor with intermittent moderate to high flooding.	Organic
4	Singh (2016b)	Talcher coalfield	Micropetrography	Peat accumulation in the forest mire under varying oxic to anoxic conditions with good tissue preservation.	Organic
5	Gangadharan et al. (2019)	Mahanadi valley	Petrography	Deposition of coal mostly under limnic to limno-telmatic conditions. Some samples favouring the deposition of peat under open marsh settings formed inertinite-rich coal.	Organic
6	Singh et al. (2019)	Nagaur basin	Petrography, x-ray fluorescence (XRF), x-ray diffraction (XRD), Fourier Transform infrared (FT-IR)	Deposition under terrestrial oxic to marine terrestrial oxic to the sub-oxic condition	Organic and inorganic
7	Singh and Kumar (2019)	Bikaner-Nagaur basin	Petrography, proximate and ultimate analysis, XRF, FT-IR	The areas with high inertinite concentrations show periodic dry (oxic) conditions during peat accumulation. These Lignites were generated from a bog forest under ombrotrophic to mesotrophic mire conditions.	Organic and inorganic
8	Mathews et al. (2020)	Rajmahal Basin	Gas chromatography–mass spectrometry (GC–MS), inductively coupled plasma mass spectrometry (ICP-MS), isotopic study	A warm temperate to subtropical climate with fresh to brackish water bodies and a decreasing oxygen-poor environment characterised the paleoclimate. Due mostly to the ongoing sinking of the early Permian Gondwana basin, this sedimentary succession was deposited in terrestrial-marginal settings with marine impact.	Organic and inorganic
9	Biswas et al. (2021)	Makum Coalfield	XRF, XRD, Palynofacies, Petrography	The coals of the Makum Coalfield were deposited under a mildly oxic-to-anoxic deltaic forest to limnic swamp conditions.	Organic and inorganic
10	Kumar et al. (2023)	Barmer basin	Petrography, proximate and ultimate analysis, XRF, XRD	During peat accumulation, the paleoclimate was warm and humid.	Organic and inorganic

(Continues)

TABLE 1 | (Continued)

Sl No.	Author(s)	Terrain/ coalfield/basin	Methodology used	Key finding	Proxies used organic/ inorganic
11	Murthy et al. (2023)	Rajmahal Basin	Palynological studies on fossiliferous material. Macro-charcoal analysis from the Barakar Formation.	The palynoflora indicates a dominance of gymnosperms, with evidence of local to regional wildfires, suggesting that frequent disturbances in continental ecosystems characterised the paleoenvironment during the early Permian in the Barakar Formation.	Organic
12	Gopinathan et al. (2024)	Singrauli coalfield	Petrography	A wet forest swamp origin with a telmatic source and bog zone under ombrotrophic to mesotrophic hydrological conditions was suggested by petrographic indices. The existence of a freshwater environment during peat deposition was further confirmed by the correlation between macerals and total sulphur levels.	Organic
13	Pillai et al. (2024)	East Bokaro basin	Morphotaxonomy, palynology and organic geochemistry	Paleoenvironment indicates a dense forest with a warm, humid climate. Depositional conditions are characterised by fluvial settings with some marine incursions	Organic
14	Srivastava et al. (2024)	Jaintia Hills	XRD, XRF, FT-IR, proximate and ultimate analyses	These coals were accumulated in warm, humid, to semi-arid climates with reducing to severely reducing circumstances.	Inorganic
15	Panda et al. (2025)	Talcher coalfield	XRD, SEM, XRF, ICP-MS	Coal deposition has been considered to have occurred mainly in a warm, humid climate with varying oxygenating circumstances.	Inorganic
16	Wahengbam et al. (2025)	Sikkim (Eastern Himalaya)	Petrography, XRD, XRF	Organic matter (OM), fungal remains and charcoal suggest an oxidising environment. Mineral complexes suggest marine to continental settings under arid to humid climates.	Organic and inorganic

TABLE 2 | Geoscientific information from the Sohagpur coalfield.

Sl No.	Author(s)	Approach	Key findings
1	Navale and Tiwari (1967)	Palynological studies	Mostly durains constitute the coal. Comparable with Lower Gondwana units in other basins.
2	Bharadwaj and Srivastava (1970)	Spore assemblage studied from borehole coal samples	Eight coal seams were distinguished based on palynological assembelege.
3	Pareek (1987)	Microlithotypes and macerals were studied	The reflectance of coal ranges from 0.46% to 1.05%.
4	Chakrabarti (1992)	The subsidence pattern of the coalfield is studied	Characteristics of coal seam are strongly controlled by the depositional environment.
5	Ram-Awatar et al. (2004)	Palynolgical studies	Late Permian age confirmed based on palynological data, which is consistent with the middle Pali Formation in the South Rewa Basin.
6	Dhanam et al. (2013)	High-resolution seismic reflection study and Borehole sonic-log data.	The study reveals high-resolution seismic imaging of the Sohagpur Gondwana basin, indicating syn-sedimentary subsidence and faulting through the identification of steeply dipping normal faults and a thick Barakar Formation, highlighting the basin's tectonic and sedimentary history.
7	Agnihotri et al. (2016)	Megafossil study	Floral assemblage overall resembles that with the Barakar Formation from other Gondwana basins in India.
8	Gautam et al. (2016)	Palynological studies	Clear-cut assemblage zones of late Permian, early and late Triassic ages.
9	Jasper et al. (2017)	Scanning electron microscopy	Fire events in a peat-forming environment.
10	Agnihotri et al. (2018)	Palynological studies	Thick coal seams were formed in the region as a result of the presence of lush vegetation during the deposition of the Barakar Formation of the Sohagpur Coalfield.
11	Mondal et al. (2020)	Geophysical tools	Large-scale coal removal, surface blasting, and the existence of hard roof strata all contributed to the longwall roof's high microseismic activity.
12	Mondal et al. (2021)	Geochemical, geophysical and geomechanical analyses	Comment on reserve quality, properties of the roof, properties gas content
13	Modi et al. (2022, 2024)	Study of rare earth elements	Average contents of critical REEs: Y—51.49 ppm, Nd—79.34 ppm, Eu—2.67 ppm, Tb—1.71 ppm, Dy—9.76 ppm
14	Bhapkar et al. (2023)	X-ray scattering measurements and high-resolution imaging	Mesopore volume and surface area reduce with depth.
15	Kishor, Kumar, et al. (2024)	Brunauer–Emmett–Teller (BET), SEM, FT-IR and High-pressure CO_2 adsorption	Coal samples from the Sharda coal mine show multilayer adsorption.
16	Kishor, Kumar Srivastava, and Singh (2024)	Vitrinite reflectance was studied, and calculation for methane and adsorbed gas content was made.	The rank of Sohagpur coal is of high volatile bituminous A type.
17	Rathore et al. (2025)	Determination of ultimate analysis and proximate components, major and trace elements using ICP-MS. XRD, X-ray fluorescence (XRF), petrography, FTIR and scanning electron microscopy–energy dispersive spectroscopy (SEM-EDS)	Elemental study suggests that some elements like Co, Cr, Nb, Ni, V, Y and Zn are very higher amounts than World Clark Hard Coal (WCHC) values. As some of these elements are known for their toxicity, they can be a threat to the ecosystem and human health.
18	Kishor et al. (2025)	Low-pressure gas adsorption analysis, scanning electron microscopy and (FTIR)	Specific surface area = 4.679 to 21.974 m^2g^{-1}, total pore volume = 0.027 to 0.054 $cm^3 g^{-1}$. Average pore diameter = 9.834 to 26.145 nm. Pores have a high capacity to store gas.

(e.g., Ward 2002; Saikia et al. 2007; Singh et al. 2019; Kumar Srivastava et al. 2024).

Organic matter of coal is crucial to define its nature and suitability for various utilities, while inorganic matter results from coal combustion at high temperatures (Creelman and Ward 1996; Ward 2002; Singh, Singh, Singh, and Banerjee 2015). Nowadays, researchers are also focusing on the evaluation of the presence and/or extraction of Rare Earth Elements (REEs) from coal, which is an inorganic constituent for various applications (e.g., Wang et al. 2003; Fu et al. 2010; Pazand 2015; Ameh 2019; Arbuzov et al. 2019; Liu et al. 2019; Kumari et al. 2023; Banerjee et al. 2024). The sulphur present in coal also plays a vital role in its combustion. The sulphur released during combustion can become a major cause of acid rain (Nath 2021). Variation of the inorganic sulphur present in coal samples is controlled by different geologic conditions. For example, the low sulphur content in certain coals is largely attributed to the limited sulphur availability in the environment during the time of peat formation and plant growth, where a greater amount of sulphur is present due to coal overlain by the marine roof, as well as sulphur may also come from seawater sulphate in the coals (Diessel 1992).

The organic (maceral) and/or inorganic matter (mineral matter) present in coal is crucial to knowing the paleoclimate and paleodepositional conditions of the coal samples. Based on the geologic ages, Indian coals are classified into two categories: Permian and Tertiary (e.g., Singh, Singh, and Singh 2015; Srivastava et al. 2025). Previously, organic matter served as the sole means to interpret the paleoclimate and paleo-depositional environments of coal samples (e.g., Singh and Singh 1996, 2000; Singh 2016a, 2016b). More recently, researchers have started examining the inorganic components of coal (e.g., Singh et al. 2019; Srivastava et al. 2024; Panda et al. 2025). Organic matter present in the coal can determine paleoclimate and paleo-depositional conditions (e.g., Kar et al. 2022, 2025; also Paul et al. 2025). For example, excessive inertinite connotes oxic depositional conditions (Singh and Singh 1996). Similarly, the presence of different inorganic constituents also states about the paleoclimate and paleo-depositional conditions. Coal with abundant kaolinite implies a warm and humid paleoclimate that resulted from intense chemical weathering, while

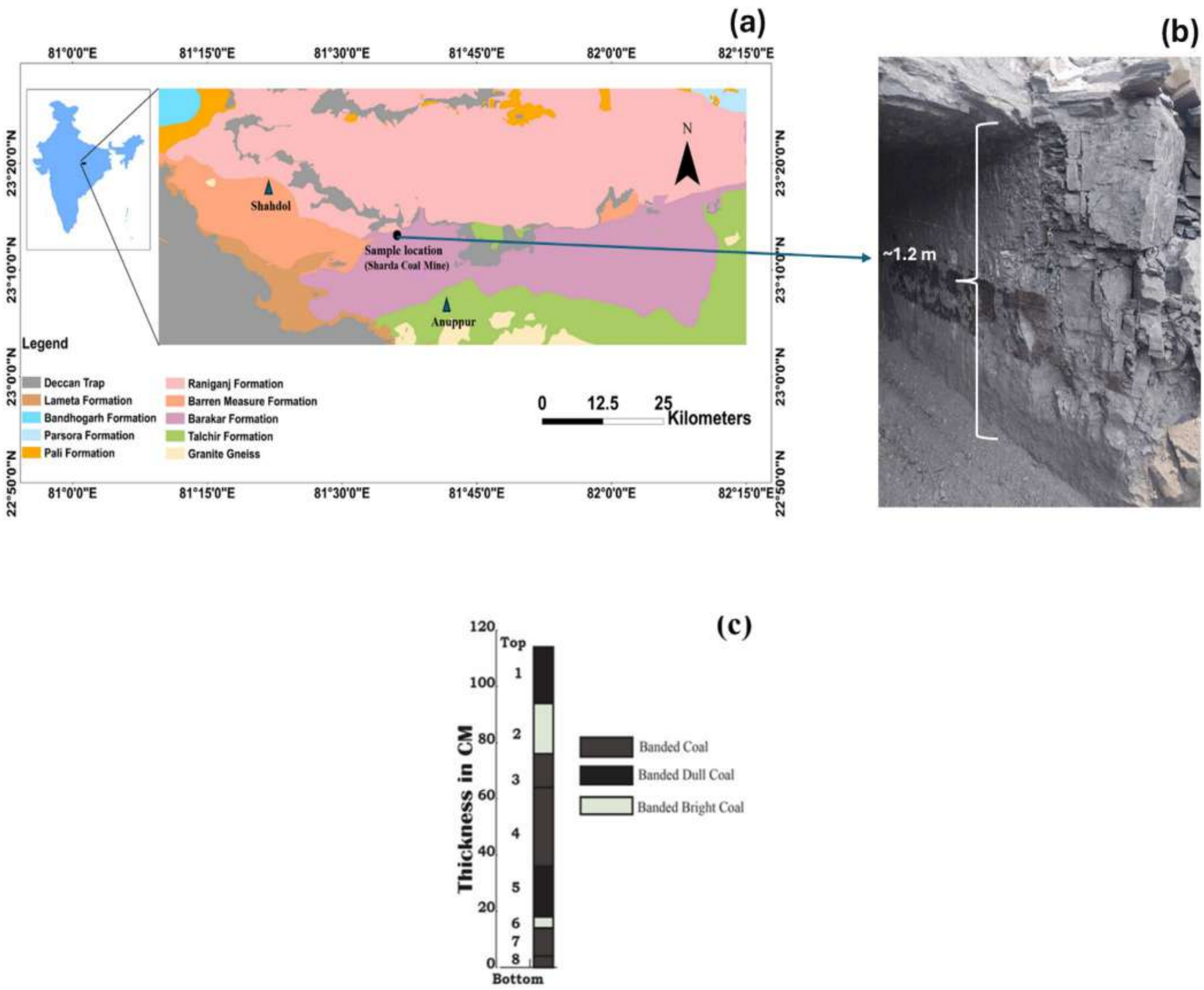

FIGURE 1 | Location map of the study area (a), Sharda mine face (Burhar Seam IV) of sample collection (b), and vertical profile section of coal samples with the thickness of each sample band (c).

a higher concentration of illite indicates a cold and arid climate. These paleoclimatic conditions were also investigated by other elemental and oxide ratios, for example, Rb/Sr and K_2O/Al_2O_3 (Roy and Roser 2013). The examination of both the entities (maceral and mineral matter) is crucial to constraining paleoclimate and paleodepositional conditions. Table 1 provides the details of several Indian authors who worked on the different terrain/basins (coal and/or lignite deposits) and deciphered the paleodepositional and paleoclimatic conditions using organic and/or inorganic proxies.

India possesses a huge coal reserve, which primarily occurs in the linearly distributed, isolated Gondwana basin and sporadic occurrences in the Himalayas. A limited literature survey has been done covering several isolated Gondwana basins in eastern and central India, and occurrences in the Himalaya (Table 1). The Sohagpur coalfield (Table 2) is located in the heartland of the coal-producing belts in central India, yet its paleoclimate and depositional environment were so far not been studied based on organic and inorganic proxies. Based on this research gap, the current research focuses on the detailed paleoclimatic and paleodepositional conditions based on the organic and inorganic proxies.

This study aims to decipher the paleoclimate and paleodepositional conditions of the Burhar Seam IV of Sharda coal mine from Sohagpur coalfield using multi-proxy analysis of maceral (organic) and mineral matters (inorganic).

2 | Study Area

The Sohagpur coalfield is one of the prominent coalfields, belonging to the Permian age, and is located in the southern part of the Son-Valley basin, in the central Indian state, Madhya Pradesh. In this coalfield, coal seams are mainly found in the Barakar Formation. The other stratigraphic units of the area are Raniganj, Pali, Parsora Formations and Barren Measures (Acharyya 2018). Sedimentary strata in this coalfield are ~1000 m thick and lie over the Precambrian basement rocks (Pareek 1987; Kishor, Kumar Srivastava, et al. 2024).

3 | Methodology

3.1 | Sample Location, Collection & Preparation

For the present study, Sharda coal open-cast mine was chosen, where the coal seam associated with the Barakar Formation belongs to the lower Gondwana Supergroup (Figure 1a). In this study, 8 coal samples were collected from the top to the bottom of the mine face to maintain the total vertical profile from seam IV of Sharda coal mine, as shown in Figure 1b. The coal seam is sandwiched between the sandstones. The vertical section of the sample collection with a thickness is shown in Figure 1c.

The sample was collected using the following Indian standards, which describe the pillar sampling technique (IS:436 1964). Coal samples were kept in zip-lock bags to avoid moisture. In the laboratory, each sample has been studied according to Diesel's classification scheme for macroscopic characterisation of coal samples. The samples show banded, banded dull and banded bright natures. After that, samples were crushed and powdered in different mesh sizes for further analysis. Figure 2 details the methodology.

3.2 | Proximate and Ultimate Analyses

Proximate analysis has been carried out to determine the moisture, volatile matter, fixed carbon and ash yield present in coal samples. During the proximate analysis, −72 mesh size of powdered coal samples was used. Analysis was performed following the Indian standard (IS:1350 1984). An ultimate analysis has been conducted to determine carbon, hydrogen, nitrogen and sulphur percentages in the coal samples. Powdered coal samples

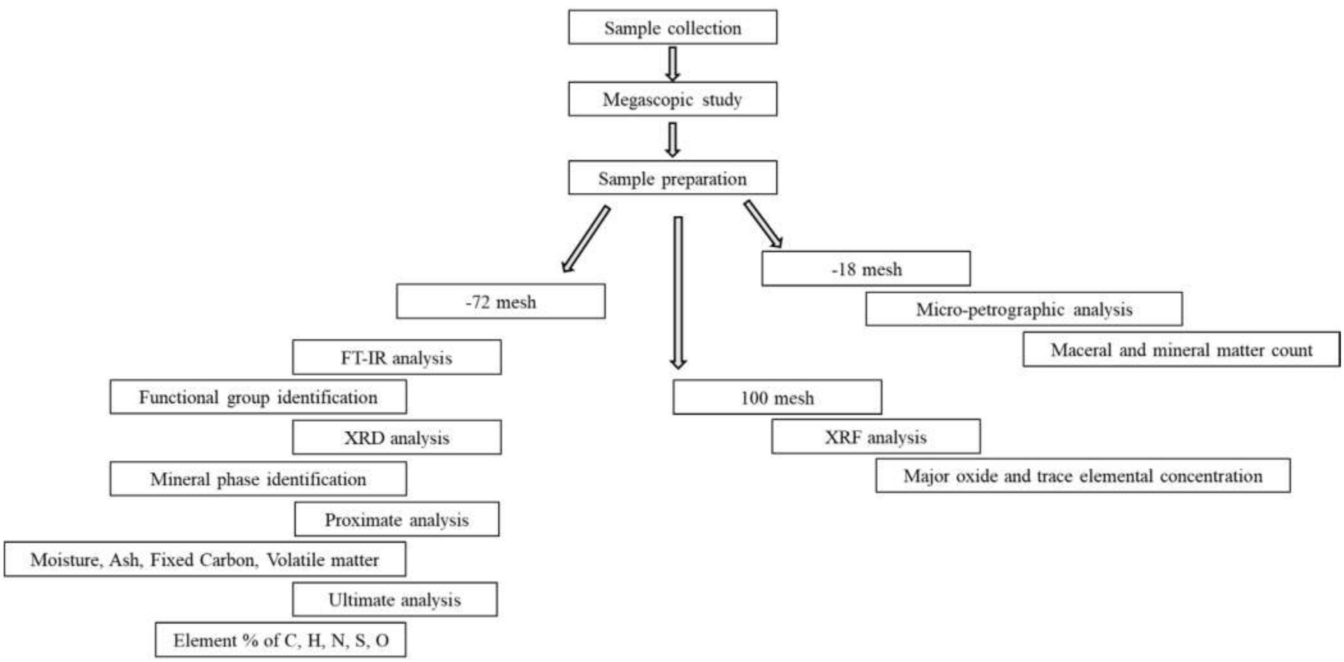

FIGURE 2 | The flowchart shows the methodology followed in this work.

of −72 mesh size were used, and a standard method of analysis was adopted (ASTM 2013).

3.3 | XRD Analysis

This preparation process was crucial, as particle size can significantly impact the results obtained from XRD, ensuring accurate identification of the various mineral phases present within the coal. The analysis was conducted over a wide angular range, specifically from 4° to 90° in the 2θ scale (θ: angle between the incident x-ray beam and the diffracted x-ray beam). This allowed a comprehensive assessment of crystal structures and mineral phases. This range was particularly effective in capturing the unique diffraction patterns that correspond to the minerals found in coal, enabling a detailed examination of its composition. For the identification of the mineral phases exhibited on the XRD chart, X'pert Highscore Plus software (v. 4.9) was used,

TABLE 3 | Coal samples and moisture, ash, volatile matter and fixed carbon % on an air-dried basis.

Sample No.	Moisture %	Ash %	Volatile matter %	Fixed carbon %
1	4.76	9.12	30.00	56.12
2	5.14	13.10	25.20	56.56
3	4.03	24.20	21.60	50.17
4	3.74	22.20	23.60	50.46
5	5.46	17.50	26.50	50.54
6	9.28	13.10	27.40	50.22
7	5.17	15.10	25.80	53.93
8	4.92	22.50	23.40	49.18
Min	3.74	9.12	21.60	49.18
Max	9.28	24.20	30.00	56.56

TABLE 4 | Coal samples and C, H, N, S % on an air-dry basis.

Sample No.	C %	H %	S %	N %
1	72.02	5.25	0.90	1.56
2	69.79	4.93	0.60	1.44
3	60.69	4.12	0.52	1.15
4	62.33	4.09	0.62	1.13
5	63.42	4.66	0.85	1.31
6	64.97	5.14	0.70	1.4
7	68.54	4.64	0.52	1.26
8	61.43	4.03	0.60	1.08
Min	60.69	4.03	0.52	1.08
Max	72.02	5.25	0.90	1.56

TABLE 5 | Oxide (%) and elemental (ppm) concentration in the studied coal samples.

Sample No.	SiO_2	Al_2O_3	K_2O	SO_3	TiO_2	MnO	MgO	CaO	K_2O	P_2O_5	Na_2O	Fe_2O_3	Rb	Sr	Cu	V	Ni	Ga
1	7.45	4.5	0.45	2.02	0.27	0.02	0.10	1.28	0.46	0.02	0.00	1.04	12.4	47.7	22.9	100.9	49.6	6.9
2	9.28	4.63	0.34	1.62	0.45	0.01	0.14	0.14	0.35	0.01	0.00	0.92	10.3	32.4	26.5	60.7	36.2	9.9
3	12.2	6.28	0.4	1.31	0.48	0.01	0.21	0.19	0.41	0.00	0.00	1.43	12.4	39.6	39.8	62	44.4	14.6
4	10.4	5.34	0.45	1.82	0.47	0.01	0.15	0.17	0.45	0.00	0.00	1.19	13	36	27.4	60.7	41.4	10.3
5	7.91	4.85	0.4	2.01	0.23	0.00	0.12	0.20	0.41	0.00	0.00	0.79	9.8	33.6	17.5	36.3	33.3	12
6	11.4	3.61	0.15	1.64	0.30	0.01	0.11	0.28	0.15	0.00	0.00	0.45	4.6	20	15.7	30.8	25.9	8.3
7	7.08	4.54	0.42	2.14	0.24	0.00	0.10	0.18	0.42	0.00	0.00	0.50	10.3	32.7	20.9	54.8	41.2	12.8
8	6.91	3.26	0.41	2.03	0.54	0.01	0.09	0.20	0.42	0.00	0.00	0.61	11.8	31.9	36.7	112.1	55	9.1
Min	6.91	3.26	0.15	1.31	0.23	0.00	0.09	0.14	0.15	0.00	0.00	0.45	4.6	20	15.7	30.8	25.9	6.9
Max	12.2	6.28	0.45	2.14	0.54	0.02	0.21	1.28	0.46	0.02	0.00	1.43	13	47.7	39.8	112.1	55	14.6

which is widely employed to analyse and match the obtained diffraction patterns with a database. The software enhances the interpretive accuracy of the data, confirming the presence of specific minerals and their abundances within coal samples. The analysis provides the mineralogic characteristics of the coal, which are pivotal for determining the paleoclimatic conditions.

3.4 | XRF Analysis

X-ray fluorescence (XRF) is a highly effective and widely used analytical tool that enables researchers to determine the concentration of various elements and oxides in a range of materials. This method is particularly valuable because it is non-destructive, meaning that the samples can be analysed without causing damage/alteration. Powdered materials of 100 mesh size were prepared. One significant characteristic of coal is its moisture content, which acts as a natural binding agent. This property allows the preparation of pressed pellets for analysis without the need for any additional additives or chemical binders. The preparation of these pellets involves using a specialised instrument designed to compress the powdered samples. This machine applies up to 25 tons of weight to ensure that the sample packs are suitable for the analysis. Once the pellets are created, XRF analysis can be performed. The results obtained from the XRF analysis were further used to determine the paleoclimate and paleodepositional conditions of the coal samples.

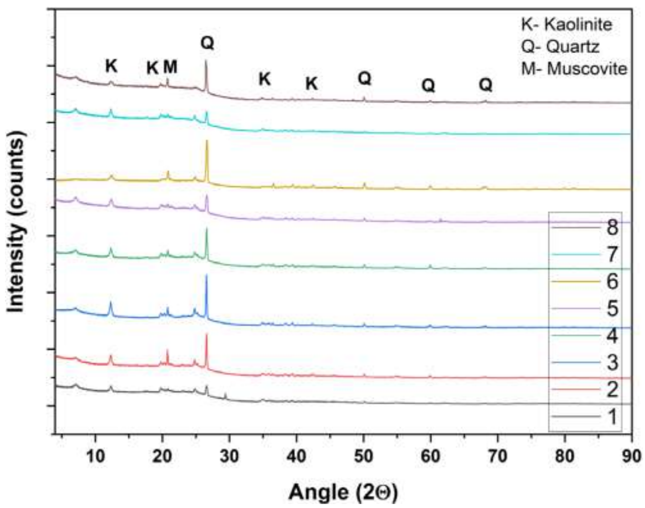

FIGURE 3 | Peaks indicate the presence of various minerals in coal samples. Major minerals and their peaks are presented. K—kaolinite, M—muscovite, Q—quartz.

3.5 | FT-IR Analysis

Fourier transform infrared (FT-IR) techniques are employed extensively to identify organic and inorganic functional groups present in coal samples. This method provides valuable insights into the chemical composition of coal, which is essential for its assessment. Coal samples were first powdered to a −72 mesh size for the FT-IR analysis and mixed with potassium bromide (KBr). KBr serves as a transparent medium that does not absorb infrared radiation. The KBr-coal mixture was pressed into a pellet to prepare the samples for analysis. The pressing process ensures that the mixture is dense and uniform, resulting in a transparent pellet that is suitable for FT-IR measurements. The FT-IR data were recorded in the transmittance mode across a 400 to 4000 cm^{-1} spectral range. Within this range, various peaks were identified, each corresponding to specific functional groups present in the coal samples. Peaks in this range were further matched with the respective inorganic functional groups of the coal samples (Estep et al. 1968; Painter et al. 1981, 1985; Chen et al. 2015).

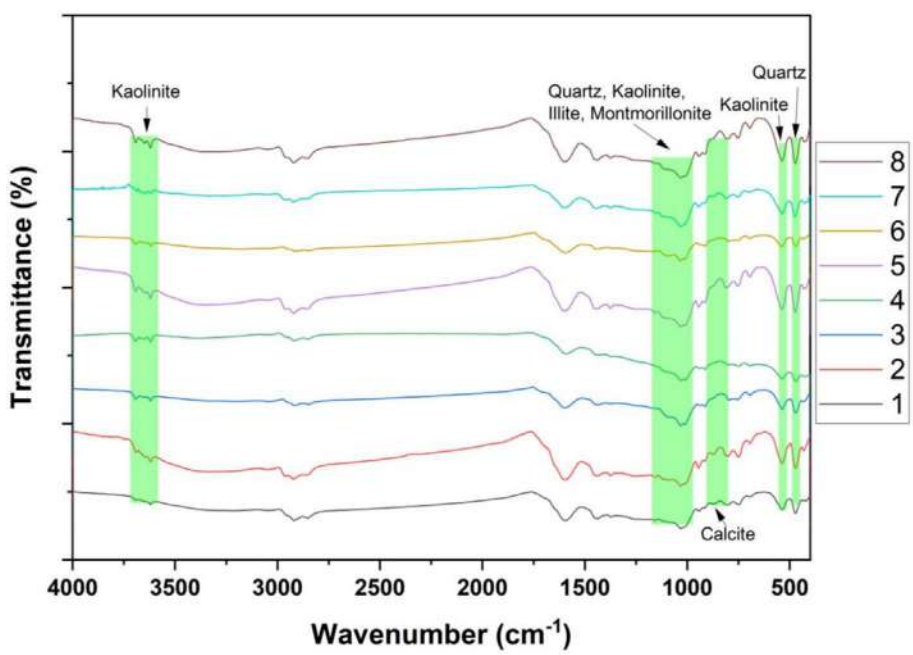

FIGURE 4 | Transmittance peaks present the inorganic functional groups present in the coal samples (shown as light green shadow).

3.6 | Micropetrography

Micropetrographic analysis was conducted on coal mounts that were explicitly prepared using −18 mesh size samples mixed with resin and hardener. This process is crucial because it allows detailed examination of the coal's microstructure, which can provide valuable insights into its properties. After the liquid mixture was poured into a mould, it solidified, forming a stable mount suitable for further analysis. The coal mount was polished to achieve a clear and scratch-free surface for microscopic examination. This involved using various grades of sandpaper and soft cloths to refine the surface until it was perfectly smooth, eliminating any imperfections that might interfere with the observations under the microscope. A reflected light microscope was employed to identify and classify macerals and mineral matter in the coal samples. The microscope was equipped with a fluorescent attachment that operated in an immersion oil medium, which enhanced visibility and contrast, enabling efficient identification. The specific model used for this analysis was a Leica microscope (DM2700P) coupled with the Leica Application Suite (Version 4.6). During the examination, macerals and mineral matter were identified using a spacing of 0.4 mm throughout the samples. This systematic approach ensures that the analysis is thorough and representative of the entire sample, enabling accurate interpretations of the coal's composition and characteristics. Throughout this process, standard procedures widely recognised in the field of coal geology were carefully adhered to in order to identify macerals under the microscope. These established protocols are critical for ensuring the reliability and validity of the results, contributing to a better understanding of coal properties and their implications in various applications (ICCP 1998, 2001; ISO 11402 2004; Pickel et al. 2017).

4 | Results

4.1 | Proximate and Ultimate Analyses

The proximate analysis result shown in Table 3 represents that the moisture content ranges from 3.74% to 9.28%, volatile matter within 21.60 and 30.00%, fixed carbon ranges from 49.18% to 56.56% and ash yield within 9.12% and 24.20% on an air-dried basis. The ultimate analysis was done to measure the sulphur present in coal samples. The C, H, N and S percent of the respective samples are shown in Table 4. Total sulphur percent is an essential parameter for deciphering the paleodepositional conditions of coal samples. The sulphur percent in these coal samples ranges from 0.52% to 0.90%.

4.2 | XRF Study

The major oxide results, SiO_2 ranges from 6.91% to 12.19%, Al_2O_3 ranges from 3.26% to 6.28% while K_2O ranges from 0.15% to 0.45% while Rb from 4.6 to 13 ppm, Sr from 20 to 47.7 ppm, Cu from 15.7 to 39.8 ppm, V from 30.8 to 112.1 ppm, Ga from 6.9 to 14.6 ppm and Ni from 25.9 to 55 ppm. Na_2O

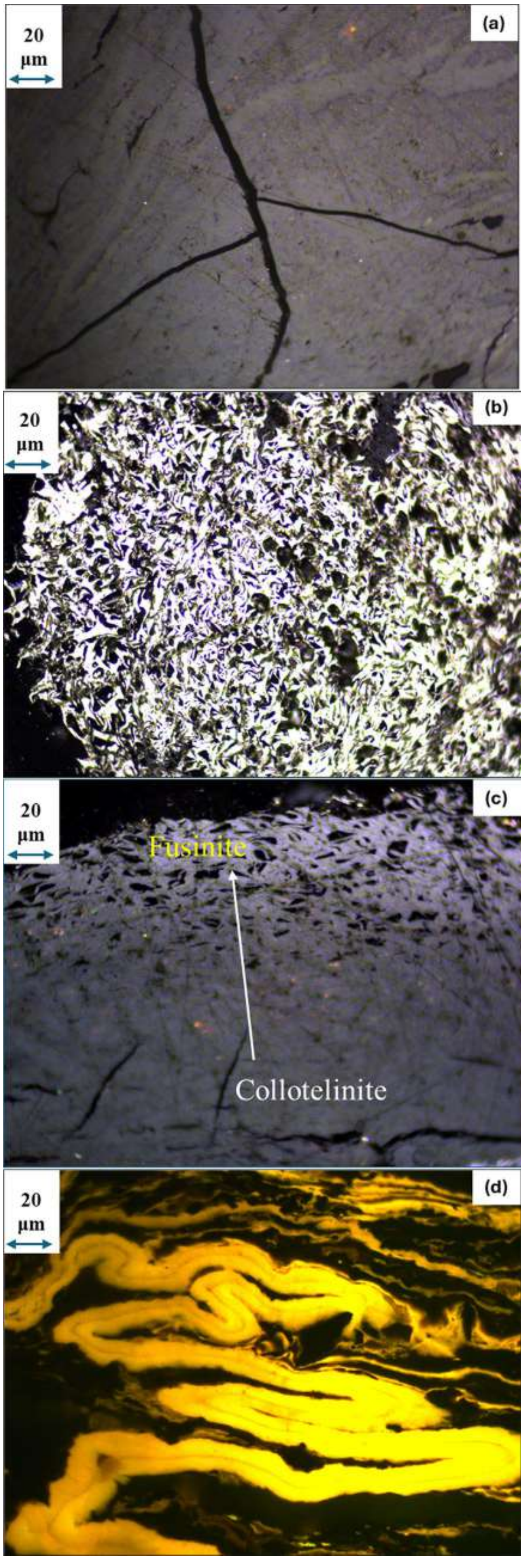

FIGURE 5 | Microphotograph of macerals present in the coal samples: a—collotelinite; b—semifusinite; c—transition from collotelinite to fusinite; d—megaspore under the fluorescent light.

deficiency in these samples is attributed to the inherently low sodium content in coal, which reflects the limited presence of sodium in the sedimentary environments where coal originates. Additionally, most sodium in coal is present in the form of soluble salts, which are often lost during the coalification process. Therefore, coal lacks significant amounts of Na_2O compared to other oxides like SiO_2 or Al_2O_3. Based on the result obtained through XRF analysis, the various cross-plots have been plotted to decipher the paleoenvironmental and paleoclimatic conditions. Table 5 shows the results of the oxides and elements required for the analysis.

4.3 | XRD Study

There is a long history of using XRD to investigate the minerals found in coal (Dai et al. 2021). The diffracted X-ray peaks height and location in the diffractogram enable identification of the inorganic components in coal, as most of them have a crystalline structure (Dai et al. 2021). XRD analysis was done between 4° and 90° of the angle of diffraction for the mineral's phase identification. The software X'pert Highscore plus software (Version 4.9) was used for the identification of mineral phases, and the graph was plotted on the Origin software (learning student version 2024). Various peaks present in the XRD graph of these coal samples show the presence of kaolinite, quartz and muscovite. These are the major mineral phases present in these coal samples. Figure 3 shows the mineral peaks identified in the XRD analysis.

4.4 | FT-IR Analysis

FT-IR analysis helps recognise various inorganic and organic functional groups that occur in coal samples. The analysis was performed for the wave number range between 400 and 4000 cm^{-1} in the transmittance mode (Figure 4). The various peaks have been identified between these wave numbers. Only inorganic functional group peaks were considered in this study

TABLE 6 | Micropetrography indicates maceral and mineral matter percentages in coal samples.

Sample No.	Tl	Cl	Vt	Cd	Cg	G	DV	PV	V	Sp	Ct	Rs	Ag	Sb	Lt	Fl	Exd
1	0	37.9	2.6	0.6	0.6	0	0	0.2	42	4.1	2.2	0.3	0	0	0.2	0	0
2	0	11.2	15.5	0	0	0	0	0.2	26.9	1.5	3	0.2	0	0	0.6	0	0.7
3	0.3	39.4	2.1	0.4	0.1	0	0	1.6	43.9	5.7	3.8	0.4	0	0	0.4	0	0.3
4	0	32.1	12.4	0.2	0.1	0	0	2	46.9	5.6	3	0.3	0	0	0.7	0	1.1
5	0	35.4	3.8	0.2	0	0	0	4.7	44.1	6.7	3.6	0.2	0	0	0.2	0	0.9
6	0	37.2	2.8	0.3	0	0	0	3	43.3	5.3	5	1.5	0.3	0	0.2	0.2	1.4
7	0.3	43.3	2	0.3	0	0.1	0	0.3	46.1	9.2	5.3	1.2	0.4	0	0.5	0	2.2
8	0	25.2	10.5	0.5	0	0	0	0.5	36.7	2.3	3.5	0.5	0	0	0.4	0	0.5
Min	0	11.2	2	0	0	0	0	0.2	26.9	1.5	2.2	0.2	0	0	0.2	0	0
Max	0.3	43.3	15.5	0.6	0.6	0.1	0	4.7	46.9	9.2	5.3	1.5	0.4	0	0.7	0.2	2.2

Sample No.	Bt	P	L	Mi	Ma	Sf	Fu	Se	It	I	Arg	Cb	Py	MM	V_{mmf}	L_{mmf}	I_{mmf}
1	0	0	6.8	0.2	0.5	17.3	1.7	6.1	7.9	33.8	14.2	2.4	0.8	17.3	50.8	8.2	40.9
2	0	0	6.1	2.2	1.2	23.1	5.7	1.2	12.8	46.1	13.5	5	2.4	20.9	34	7.7	58.3
3	0	0	10.6	0.2	0.8	9.6	12.7	2.5	8	33.8	9	1.9	0.7	11.7	49.7	12	38.3
4	0	0	10.6	0	0.3	6.9	9	3.9	7.2	27.2	13.2	1.2	1	15.3	55.3	13	32.1
5	0	0	11.7	0.1	1.2	9.3	5.5	8.2	9.8	34.2	7.2	1.9	1	10.1	49	13	38
6	0	0	13.9	0.3	0.8	8.8	3.2	2.5	15	30.7	7.5	2.8	1.8	12.1	49.3	16	34.9
7	0.3	0	19	0.3	0.6	7.9	3.4	4	5	21.2	8.7	3.3	1.6	13.7	53.4	22	24.6
8	0	0	7.3	0.2	0.7	28.6	5.6	2.3	9.3	46.7	6.5	2.4	0.3	9.2	40.4	8.1	51.5
Min	0	0	6.1	0	0.3	6.9	1.7	1.2	5	21.2	6.5	1.2	0.3	9.2	34	7.7	24.6
Max	0.3	0	19	2.2	1.2	28.6	12.7	8.2	15	46.7	14.2	5	2.4	20.9	55.3	22	58.3

Abbreviations: Ag, alginite; Arg, agrillaceous mineral matter; Bt, bituminite; Cb, carbonate mineral matter; Cd, collodetrinite; Cg, corpogellinite; Cl, collotelinite; Ct, cutinite; DV, dark vitrinite; Exd, exsudatinite; Fl, fluorenite; Fu, fusinite; G, gelinite; I, inertinite; I_{mmf}, inertinite on mineral matter free basis; It, inertodetrinite; L, liptinite; L_{mmf}, inertinite on mineral matter free basis; Lt, litrodetrinite; Ma, macrinite; Mi, micrinite; MM, mineral matter; P, pollen; PV, pseudo vitrinite; Py, pyrite; Rs, resinite; Sb, suberinite; Se, secretinite; Sf, semifusnite; Sp, sporinite; Tl, telinite; V, vitrinite; V_{mmf}, inertinite on mineral matter free basis; Vt, vitrodetrinite.

to focus on the mineral components of the coal. The peaks within 3600 to 3700 cm^{-1} show the occurrence of kaolinite, which falls under the inorganic functional group. Similarly, the peaks in the range of 400 to 1100 cm^{-1} come under the inorganic functional group, which includes various minerals, for example, kaolinite, illite, montmorillonite, calcite and quartz (Estep et al. 1968; Chen et al. 2015; Equeenuddin et al. 2016; Srivastava et al. 2024).

4.5 | Micropetrographic Study

Coal macerals are divided into three groups as follows: (1) Liptinite group macerals- these are comparatively rich in hydrogen, (2) vitrinite group macerals- these are relatively rich in oxygen and (3) inertinite group macerals differ chemically from the previous ones because they are substantially carbon-rich (Singh and Singh 2004). As per the International Committee for Coal and Organic Petrology (ICCP) recommendation and International Organisation for Standardisation (ISO) norms (ICCP 1998, 2001; ISO 11402 2004; Pickel et al. 2017), micropetrographic analysis was performed to identify organic (maceral) and inorganic (minerals) matters. Liptinite maceral groups were identified under the microscope attached to fluorescent irradiation (Teichmuller and Wolf 1977). Figure 5 presents the representative microphotograph of the coal macerals identified under the white and fluorescent light.

Petrographic result shows that vitrinite is a dominant maceral group, which ranges from 26.9% to 46.9%, followed by inertinite (21.2%–46.7%) and liptinite (6.1%–19.0%). The mineral matters range from 9.2% to 20.9%. Additionally, the maceral values on a mineral matter-free (mmf) basis have also been calculated (Table 6).

5 | Discussion

5.1 | Paleoclimatic Conditions

The rate of chemical weathering of rocks is controlled by several factors, including climate, the composition of the source rock and the tectonic setting (Mikheeva et al. 2021). A combination of XRF, XRD and FT-IR results gives an idea of the paleoclimatic conditions of coal samples. Major oxide results obtained through XRF analysis and cross-plots proposed by Suttner and Dutta (1986), followed by Mortazavi et al. (2014), Singh et al. (2019), Tchouatcha et al. (2023) and so forth show that all the samples fall within the warm/humid paleoclimate (Figure 6a). The Ga/Rb vs. K_2O/Al_2O_3 cross-plot shows that the environment was warm and humid (Figure 6b). Since samples that are rich in illite have higher values of K_2O/Al_2O_3 and lower values of Ga/Rb, while the samples rich in kaolinite show the opposite pattern with higher values of Ga/Rb and lower values of K_2O/Al_2O_3. In the case where the value of Rb/Sr is high, the climate was cold, while a lower value of this ratio represents a warmer climate (e.g., Bai et al. 2015; Jin and Zhang 2002). For the analysed samples, the Rb/Sr ratio is relatively low. This connotes a warm and humid paleoclimate (Figure 6c). The XRD and FT-IR analyses, which identify mineral phases and inorganic functional groups, suggest that kaolinite is abundantly present in these coals, since the formation of kaolinite is done by the intense chemical weathering of feldspar under warm and humid climatic conditions; the presence of this mineral favours that coal was formed during warm and humid paleoclimatic conditions (Figures 3 and 4).

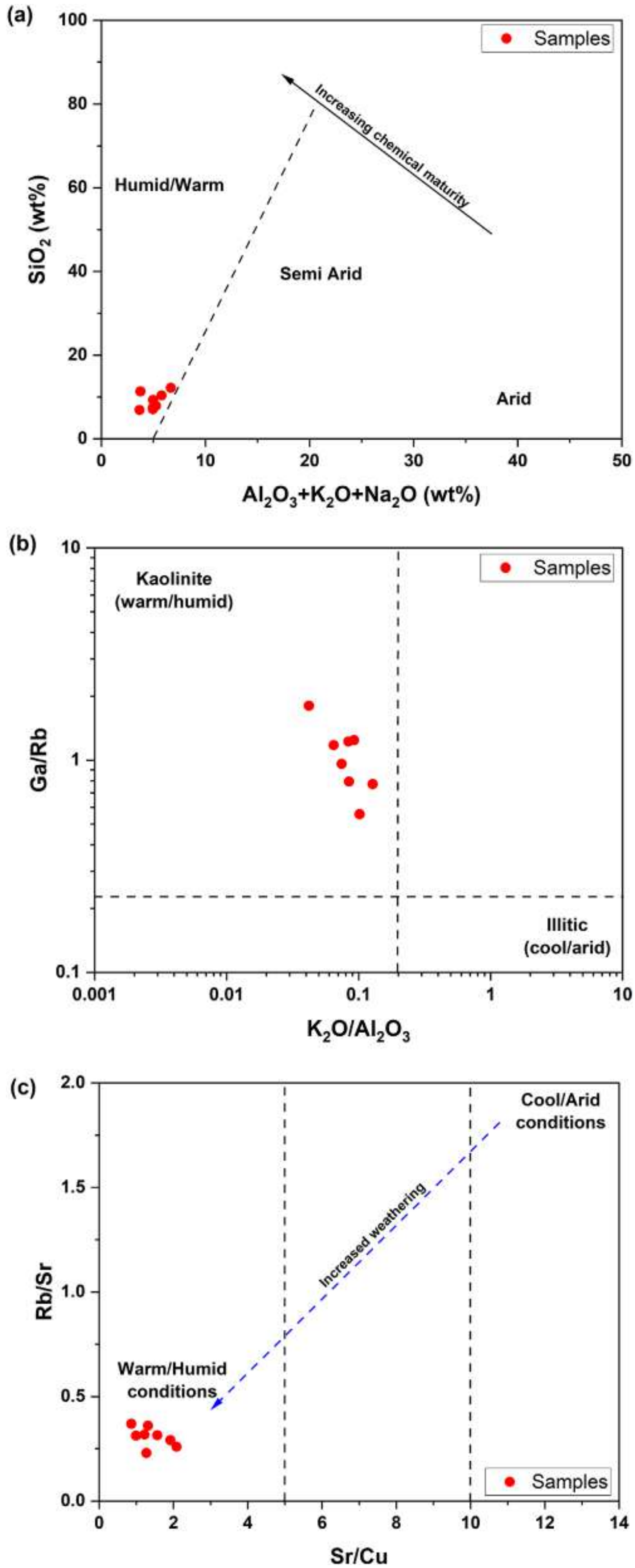

FIGURE 6 | Different cross-plots show that the paleoclimatic conditions of coal samples (a) cross-plot SiO_2 versus ($Al_2O_3 + K_2O + Na_2O$), (b) Ga/Rb vs. K_2O/Al_2O_3; (c) Rb/Sr versus Sr/Cu cross-plots show the climatic conditions were warm/humid.

5.2 | Paleo-Depositional Conditions

Cross-plot of V vs. Al_2O_3 suggests that the depositional conditions of the coal samples were predominantly influenced by environments transitioning between fluvial systems and shallow marine settings (Figure 7a). Another cross-plot explores the V vs. Ni relationship (Figure 7b), which serves as an essential parameter for understanding paleo deposition. The cross-plot derived from this analysis indicates that the coal samples from the Burhar Seam IV were deposited in conditions ranging from terrestrial oxic (well-aerated and suitable for organic decomposition) to marine–terrestrial oxic, suboxic environments (areas with reduced oxygen levels that can affect organic matter accumulation). Another cross-plot (Figure 7c) supports the interpretation that correlates V/(V + Ni) with the total sulphur content. The results from this plot suggest that the coal samples were deposited in suboxic conditions. This reflects a complex interplay among different depositional environments. The findings suggest that coal samples were deposited in environment with oxic to suboxic redox conditions.

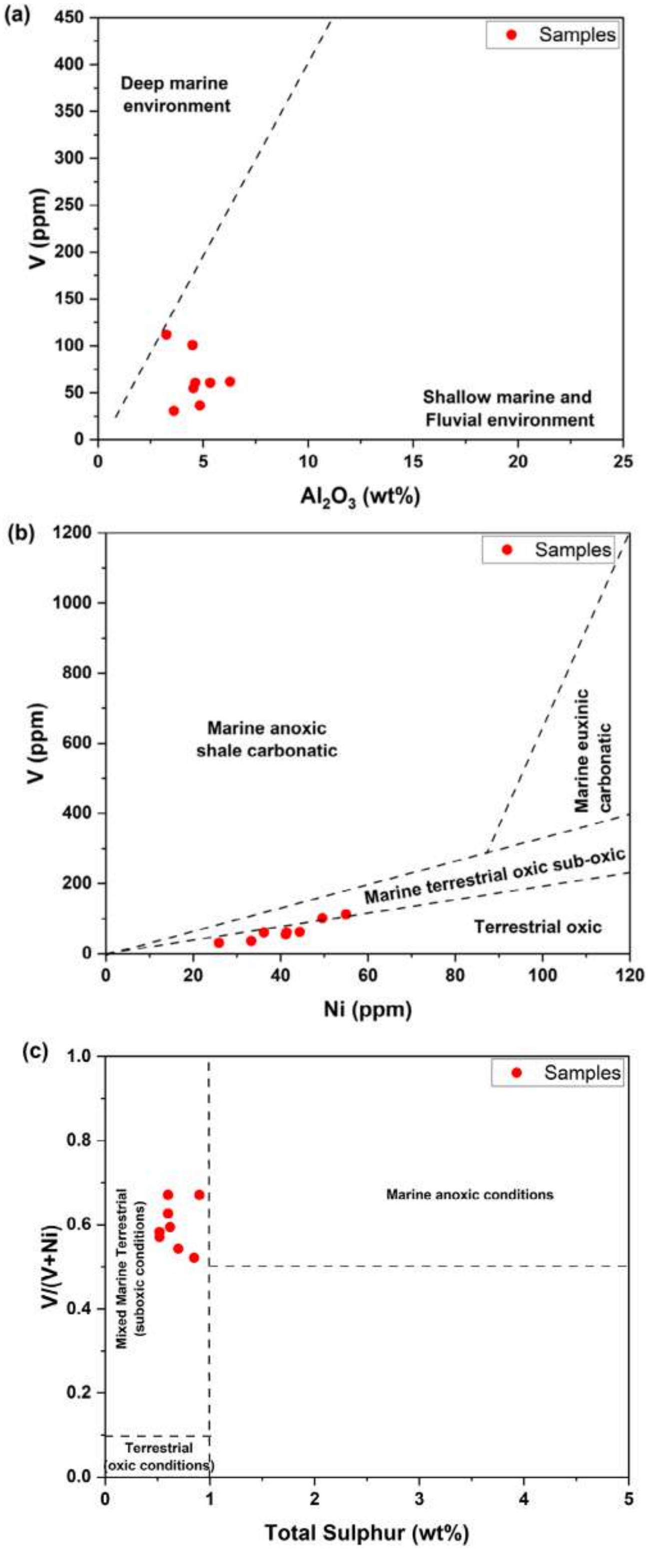

FIGURE 7 | Cross-plots showing the paleo-depositional conditions of coal samples. (a) Al_2O_3 versus V (Mortazavi et al. 2014) (b) V versus Ni (Galarraga et al. 2008), (c) total sulphur versus V/(V + Ni).

Based on the micropetrographic data (Table 7), we attempt to decipher the paleodepositional conditions of the coal samples. Two depositional models were plotted as per Singh and Singh (1996) and Mukhopadhyay (1986) in Figure 8a,b.

Singh and Singh (1996) proposed a model that effectively illustrates the paleo-depositional conditions of coal samples. This model was proposed based on data obtained from the coals of the Rajmahal Basin, which is also a part of the lower Gondwana Group. The triangular plot utilises maceral and mineral matter data, which encompasses three key components: vitrinite + liptinite, Inertinite and mineral matter (Figure 8a). Vitrinite + liptinite content ranges from 33.0% to 65.1%. Inertinite values fall between 21.2% to 46.7%, while the mineral matter ranges from 9.2% to 20.9%. A comprehensive dataset of Sohagpur coals used in this triangular plot is provided in Table 7. When the maceral and mineral matter data were plotted on this triangular graph, an interesting pattern emerged—every sample point was located within the D zone, indicating alternating oxic (oxygen-rich) and anoxic (oxygen-deficient) environments found in moor settings.

Maceral and sub-maceral data obtained from micropetrography were plotted in Figure 8b. This plot has been widely used by

TABLE 7 | Organic and inorganic entities (%) present in coal samples.

Sample No.	V + L	I	MM	A	B	C
1	48.8	33.8	17.3	54.4	4.2	41.4
2	33.0	46.1	20.9	20.4	20.6	59.0
3	54.5	33.8	11.7	57.6	3.1	39.3
4	57.5	27.2	15.3	50.4	16.2	33.4
5	55.7	34.2	10.1	54.6	4.7	40.6
6	57.3	30.7	12.1	59.3	3.6	37.1
7	65.1	21.2	13.7	71.4	3.0	25.6
8	44.0	46.7	9.2	35.3	12.2	52.4
Min	33.0	21.2	9.2	20.4	3.0	25.6
Max	65.1	46.7	20.9	71.4	20.6	59.0

Abbreviations: A: telinite + collotelinite + sporinite + cutinite + resinite, B: vitrodetrinite + liptodetrinite + gelocolinite, C: inertinite, I: inertinite, L: liptinite, MM: mineral matter, V: vitrinite.

several researchers for the determination of paleodepositional conditions of coal (e.g., Singh and Singh 1996, 2000; Singh 2016b; Biswas et al. 2021, 2024). The value of A ranges from 20.4% to 71.4%, B from 3.0% to 20.6% and C from 25.6% to 59.0% (Table 7). Here as well, plots fall mainly in the D zone. This indicates that coal samples deposited in a forest swamp, mildly oxic to anoxic, whereby tissues got well preserved.

From both the models (Figure 8), it is evident that the vegetal matter accumulated in the forested swamps with fluctuating water levels gave rise to alternate oxic and anoxic conditions, with good tissue preservation. The inertinite may derive from the fire in the peat (Jasper et al. 2017) or degradation of plant tissue in the oxic condition (Shi et al. 2024), whereas collotelinite forms when the tissue preservation is good (ICCP 1998). In this case, the abundance of inertinite with a gradational change in a single grain, from collotelinite to semifusinite and finally to fusinite, was observed (Figure 5c). This might have resulted from the oxidation of the outer surface of the plant tissue, whereas the preservation of the inner or lower part of the same tissue. Hence, an alternate oxic and anoxic condition might have developed in the mire. This condition might arise due to the mixing of oxygenated water in the anoxic swamp water, which indicates a seasonal flooding of the basin.

From the petrography, it is evident that this coal is dominated by inertinite and vitrinite. Nandi et al. (1977) stated that the inert maceral is inversely proportional to combustion

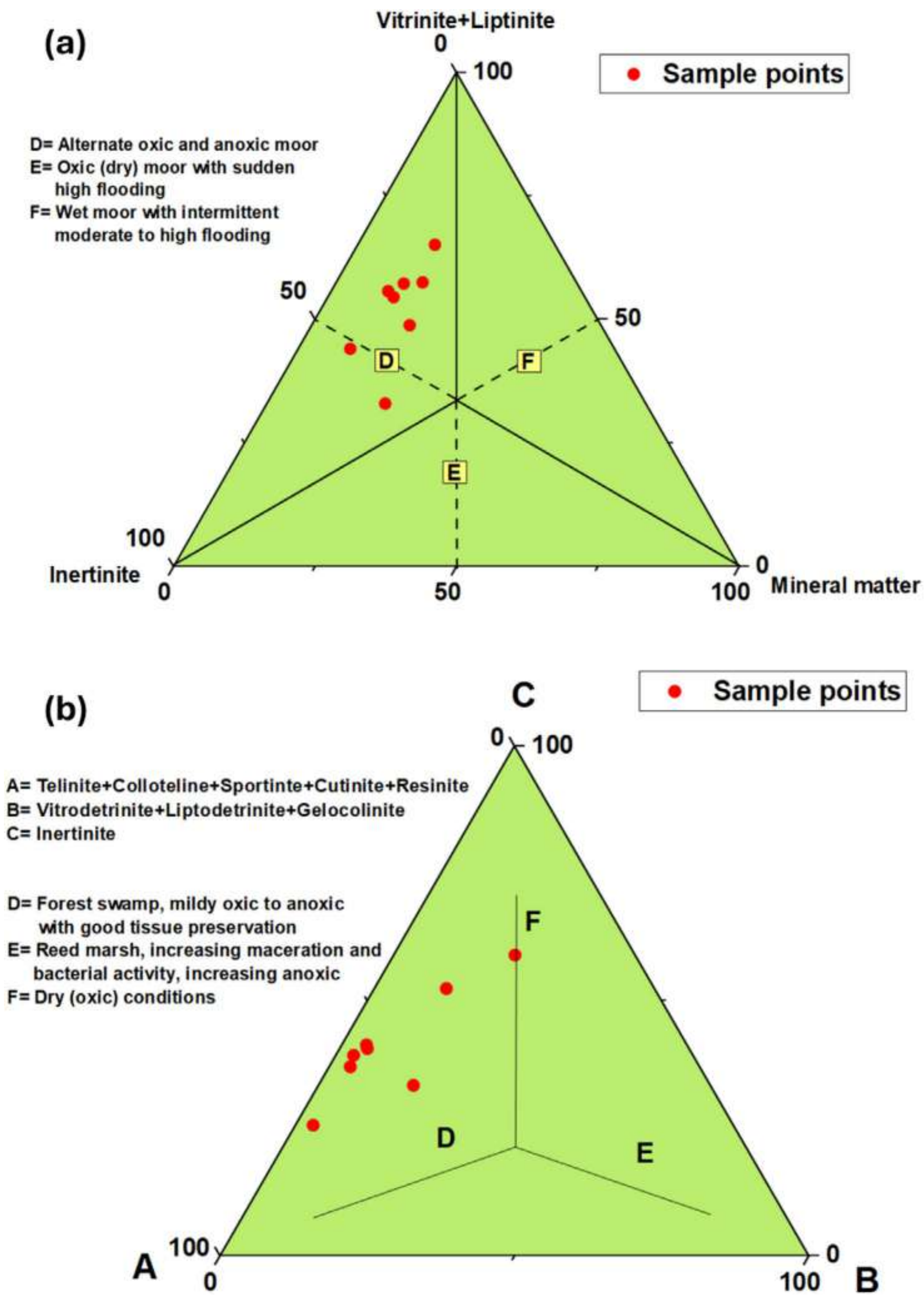

FIGURE 8 | (a) The triangular plot of maceral and mineral matter (after Singh and Singh 1996) shows the depositional conditions of coal samples. (b) The triangular plot (Mukhopadhyay 1986) based on the maceral subgroup also indicates the same depositional conditions of coal samples.

efficiency. The maceral groups also affect the CO_2 adsorption in coals; vitrinite-rich coals show higher efficiency in CO_2 adsorption due to micropore abundance (Premlall and Koech 2025). Proximate analysis shows that these coals are rich in ash yield. The inferred depositional model suggests that peat swamps suffered from seasonal flooding, which might have facilitated the influx of mineral matter into the swamp. These detrital mineral matters can be a source of REEs in coal.

6 | Conclusions

The multi-proxies and multi-analytical analyses present the paleoclimate and paleo-depositional conditions of coal samples from the Sharda coal mine. XRD, XRF and FT-IR analysis results show that during the deposition, the climatic conditions were warm and humid. Similarly, the ultimate analysis, XRF and micropetrography data were used to determine the paleo-depositional conditions. The analysis of XRF and ultimate analysis data shows that coal samples were deposited in a transitional setting of oxic to suboxic conditions. Micropetrographic analysis also shows that coal samples were deposited in alternating oxic to anoxic moor and mildly oxic to anoxic with good tissue preservation. Combining inorganic and organic proxies is essential to decipher the paleodepositional and paleoenvironmental conditions of coal samples, as Table 2 suggests that the Sohagpur coalfield has never been examined through these proxies for paleoenvironmental and paleodepositional conditions.

Author Contributions

All authors contributed to this study. K.K. collected and analysed samples and wrote the first draft. M.K.S. and G.P.T. analysed samples and revised and edited the manuscript. S.M. edited and reviewed the manuscript while A.K.S. conceptualised, supervised and finalised the manuscript.

Acknowledgements

We thank the Director, Rajiv Gandhi Institute of Petroleum Technology (RGIPT), for providing facilities. We appreciate the Southeastern Coalfield (SECL) for assistance in collecting the coal samples.

Conflicts of Interest

The authors declare no conflicts of interest.

Data Availability Statement

Data are provided within the manuscript.

References

Acharyya, S. 2018. *Tectonic Setting and Gondwana Basin Architecture in the Indian Shield*, edited by S. Mukherjee, vol. 4. Elsevier.

Agnihotri, D., S. Pillai, N. Aggarwal, R. Tewari, A. Jasper, and D. Uhl. 2018. "Palynomorphs From the Barakar Formation of Dhanpuri Open Cast Mine, Sohagpur Coalfield, Madhya Pradesh, India." *Journal of Palaeosciences* 67, no. 1-2: 171–184. https://doi.org/10.54991/jop.2018.56.

Agnihotri, D., R. Tewari, S. S. K. Pillai, A. Jasper, and D. Uhl. 2016. "Early Permian Glossopteris Flora From the Sharda Opencast Mine, Sohagpur Coalfield, Shahdol District, Madhya Pradesh." *Journal of Palaeosciences* 65: 97–107. https://doi.org/10.54991/jop.2016.302.

Ameh, E. G. 2019. "Geochemistry and Multivariate Statistical Evaluation of Major Oxides, Trace and Rare Earth Elements in Coal Occurrences and Deposits Around Kogi East, Northern Anambra Basin, Nigeria." *International Journal of Coal Science & Technology* 6: 260–273. https://doi.org/10.1007/s40789-019-0247-4.

Arbuzov, S. I., D. A. Spears, A. V. Vergunov, et al. 2019. "Geochemistry, Mineralogy, and Genesis of Rare Metal (Nb-Ta-Zr-Hf-Y-REE-Ga) Coals of the Seam XI in the South of Kuznetsk Basin, Russia." *Ore Geology Reviews* 113: 103073. https://doi.org/10.1016/j.oregeorev.2019.103073.

ASTM. 2013. "D 3176–89 Standard Practice for Ultimate Analysis of Coal and Coke." *Methods* 89: 3178–3180.

Bai, Y., Z. Liu, P. Sun, et al. 2015. "Rare Earth and Major Element Geochemistry of Eocene Fine-Grained Sediments in Oil Shale- and Coal-Bearing Layers of the Meihe Basin, Northeast China." *Journal of Asian Earth Sciences* 97: 89–101. https://doi.org/10.1016/j.jseaes.2014.10.008.

Banerjee, R., S. Chakladar, A. Kumar, S. K. Chattopadhyay, and S. Chakravarty. 2024. "Petrology and Association of Rare Earth Elements in Magmatically Altered High-Ash Coal of Indian Origin." *International Journal of Coal Science & Technology* 11: 52. https://doi.org/10.1007/s40789-024-00709-6.

Bhapkar, P. V., S. P. Pradhan, D. Chandra, B. Hazra, and V. Vishal. 2023. "Systematic Pore Characterization of Sub-Bituminous Coal From Sohagpur Coalfield, Central India, Using Gas Adsorption Coupled With X-Ray Scattering and High-Resolution Imaging." *Energy & Fuels* 37: 9297–9308. https://doi.org/10.1021/acs.energyfuels.3c01007.

Bharadwaj, D. C., and S. C. Srivastava. 1970. "Sporological Correlation of Coal Seams in Some Blocks of Sohagpur Coalfield, MP, India." *Journal of Palaeosciences* 19: 1–28. https://doi.org/10.54991/jop.1970.851.

Biswas, S., A. K. Varma, M. Kumar, and B. K. Saikia. 2021. "Multi-Analytical Approach of Provenance Signatures and Indication of Marine Environment in Coal and Shale Bearing Sequence From Makum Coalfield, India." *Arabian Journal of Geosciences* 14: 2183. https://doi.org/10.1007/s12517-021-08569-z.

Biswas, S., N. J. Wagner, and O. M. Moroeng. 2024. "Organic Petrographic and Mineralogical Composition of the No. 6 Coal Seam of the Soutpansberg Coalfield, South Africa: Insights Into Paleovegetation and Depositional Environment." *International Journal of Coal Science & Technology* 11: 41. https://doi.org/10.1007/s40789-024-00698-6.

Chakrabarti, U. 1992. "Intrabasinal Differential Subsidence and Its Influence on Coal Thickness Configuration, Barakar Formation, Sohagpur Coalfield, Madhya Pradesh." *Journal Geological Society of India* 39: 212–222.

Chen, Y., C. Zou, M. Mastalerz, S. Hu, C. Gasaway, and X. Tao. 2015. "Applications of Micro-Fourier Transform Infrared Spectroscopy (FTIR) in the Geological Sciences—A Review." *International Journal of Molecular Sciences* 16: 30223–30250. https://doi.org/10.3390/ijms161226227.

Creelman, R. A., and C. R. Ward. 1996. "A Scanning Electron Microscope Method for Automated, Quantitative Analysis of Mineral Matter in Coal." *International Journal of Coal Geology* 30: 249–269. https://doi.org/10.1016/0166-5162(95)00043-7.

Dai, S., R. B. Finkelman, D. French, J. C. Hower, I. T. Graham, and F. Zhao. 2021. "Modes of Occurrence of Elements in Coal: A Critical Evaluation." *Earth-Science Reviews* 222: 103815. https://doi.org/10.1016/j.earscirev.2021.103815.

Dhanam, K., P. Senthil Kumar, D. Mysaiah, et al. 2013. "High-Resolution Seismic Imaging of the Sohagpur Gondwana Basin, Central India: Evidence for Syn-Sedimentary Subsidence and Faulting." *Journal of Earth System Science* 122: 1495–1505. https://doi.org/10.1007/s12040-013-0362-3.

Diessel, C. F. K. 1992. *Coal-Bearing Depositional Systems*. Springer Berlin Heidelberg.

Equeenuddin, S. M., S. Tripathy, P. K. Sahoo, and A. Ranjan. 2016. "Geochemical Characteristics and Mode of Occurrence of Trace Elements in Coal at West Bokaro Coalfield." *International Journal of Coal Science & Technology* 3: 399–406. https://doi.org/10.1007/s40789-016-0146-x.

Estep, P. A., J. J. Kovach, and C. Karr. 1968. "Quantitative Infrared Multicomponent Determination of Minerals Occurring in Coal." *Analytical Chemistry* 40: 358–363. https://doi.org/10.1021/ac60258a006.

Fu, X., J. Wang, Y. Zeng, F. Tan, and X. Feng. 2010. "REE Geochemistry of Marine Oil Shale From the Changshe Mountain Area, Northern Tibet, China." *International Journal of Coal Geology* 81: 191–199. https://doi.org/10.1016/j.coal.2009.12.006.

Galarraga, F., K. Reategui, A. Martïnez, M. Martínez, J. F. Llamas, and G. Márquez. 2008. "V/Ni Ratio as a Parameter in Palaeoenvironmental Characterisation of Nonmature Medium-Crude Oils From Several Latin American Basins." *Journal of Petroleum Science and Engineering* 61: 9–14. https://doi.org/10.1016/j.petrol.2007.10.001.

Gangadharan, G. K., C. P. Ramteke, and S. N. Chaudhuri. 2019. "Petrographic Studies to Delineate Suitable Coal Seams for Coal Liquefaction and Their Palaeo-Environmental Analysis: A Case Study From the Ib River and Mand-Raigarh Coalfields of the Mahanadi Valley Coalfields, India." *Journal of Earth System Science* 128, no. 6: 165. https://doi.org/10.1007/s12040-019-1180-z.

Gautam, S., R. Tewari, and S. Goswami. 2016. "Permian-Triassic Palynofloral Transition in Sohagpur Coalfield, South Rewa Gondwana Basin, Madhya Pradesh, India." *Journal of Palaeosciences* 65: 109–129. https://doi.org/10.54991/jop.2016.303.

Gopinathan, P., A. Mahato, O. P. Kumar, et al. 2024. "Evaluation of Singrauli Coals for Sustainable Energy Utilisation: Insight From Geochemical and Petrographic Perspectives." *Geological Journal*. https://doi.org/10.1002/gj.5060.

IBM. 2021. "Indian Minerals Yearbook 2021 60th Edition COAL & LIGNITE."

ICCP. 1998. "New Vitrinite Classification (ICCP System 1994)." *Fuel* 77: 349–358. https://doi.org/10.1016/S0016-2361(98)80024-0.

ICCP. 2001. "New Inertinite Classification (ICCP System 1994)." *Fuel* 80: 459–471. https://doi.org/10.1016/S0016-2361(00)00102-2.

IS:1350. 1984. "Indian Standard Methods of Test for Coal and Coke Part I Proximate Analysis (Second Revision)." Bureau of Indian Standards 28.

IS:436. 1964. "IS 436-1-1 (1964): Methods for Sampling of Coal and Coke, Part 1: Sampling of Coal, Section 1: Manual Sampling (Revised)." Bureau of Indian Standards.

ISO 11402. 2004. "Method of Determining Maceral Group Composition (ISO 7404-3)." International Organization for Standardization 10406–1:20:3–6.

Jasper, A., D. Agnihotri, R. Tewari, et al. 2017. "Fires in the Mire: Repeated Fire Events in Early Permian' Peat Forming' Vegetation of India." *Geological Journal* 52: 955–969. https://doi.org/10.1002/gj.2860.

Jin, Z. D., and E. L. Zhang. 2002. "Paleoclimate Implications of Rb/Sr Ratios From Lake Sediments." *Science, Technology and Engineering* 2, no. 3: 20–22 (in Chinese with English abstract).

Kar, N. K., D. Mani, S. Mukherjee, et al. 2022. "Source Rock Properties and Kerogen Decomposition Kinetics of Eocene Shales From Petroliferous Barmer Basin, Western Rajasthan, India." *Journal of Natural Gas Science and Engineering* 100: 104497. https://doi.org/10.1016/j.jngse.2022.104497.

Kar, N. R., D. Mani, B. S. Seetha, et al. 2025. "Biomarker Evidence of Shifts in Organic Provenance and Depositional Environments of Eocene Carbonaceous Rocks From Petroliferous Barmer Basin, Western Rajasthan, India." *Journal of the Geological Society of India* 101: 112–122. https://doi.org/10.17491/jgsi/2025/174065.

Kishor, K., M. Kumar, M. Kumar Srivastava, and A. K. Singh. 2024. "Geochemical and Microstructural Analysis of Coals From Sohagpur Coalfield With Reference to Adsorption Behaviour: An Assessment for CO_2 Sequestration." *International Journal of Coal Preparation and Utilization* 44: 941–952. https://doi.org/10.1080/19392699.2023.2232721.

Kishor, K., M. Kumar Srivastava, and A. K. Singh. 2024. "Geochemical Study of Coals From Sohagpur Coalfield, India, and Its Implication to CBM Potential." *International Journal of Coal Preparation and Utilization* 44: 614–625. https://doi.org/10.1080/19392699.2023.2212611.

Kishor, K., M. K. Srivastava, and A. K. Singh. 2025. "Pore Characteristics and Gas Adsorption Properties of Permian Coals in Sohagpur Coalfield, India: A Comprehensive Multi-Analytical Study." *Energy & Fuels* 39: 349–361. https://doi.org/10.1021/acs.energyfuels.4c04722.

Kumar, A., A. K. Singh, and K. Christanis. 2023. "Paleodepositional Environment and Hydrocarbon Generation Potential of the Paleogene Lignite in the Barmer Basin, Rajasthan, India." *Journal of Asian Earth Sciences* 259: 105892. https://doi.org/10.1016/j.jseaes.2023.105892.

Kumar Srivastava, M., K. Kishor, and A. K. Singh. 2024. "A Comprehensive Petrochemical Study of Coals of Jaintia Hills: Unveiling Their Industrial Applicability and Potential as Hydrocarbon Source Rocks." *International Journal of Coal Preparation and Utilization* 00: 1–836. https://doi.org/10.1080/19392699.2024.2353130.

Kumari, S., T. Roy, S. Chakladar, et al. 2023. "Distribution, Mode of Occurrence, and Significance of Rare-Earth Elements in Coal From Samaleswari Open Cast Coal Blocks, Odisha, India, With Their Provenance and Paleodepositional Environment." *Environment and Earth Science* 82: 130. https://doi.org/10.1007/s12665-023-10777-7.

Liu, P., L. Yang, Q. Wang, et al. 2019. "Speciation Transformation of Rare Earth Elements (REEs) During Heating and Implications for REE Behaviors During Coal Combustion." *International Journal of Coal Geology* 219: 103371. https://doi.org/10.1016/j.coal.2019.103371.

Mathews, R. P., S. S. K. Pillai, M. Manoj, and S. Agrawal. 2020. "Palaeoenvironmental Reconstruction and Evidence of Marine Influence in Permian Coal-Bearing Sequence From Lalmatia Coal Mine (Rajmahal Basin), Jharkhand, India: A Multi-Proxy Approach." *International Journal of Coal Geology* 224: 103485. https://doi.org/10.1016/j.coal.2020.103485.

Mikheeva, E. A., E. I. Demonterova, and A. V. Ivanov. 2021. "Geochemistry of the Cheremkhovo and Lower Prisayan Formations From the Jurassic Irkutsk Coal-Bearing Basin: Evidence for Provenance and Climate Change in Pliensbachian–Toarcian." *Minerals* 11: 357. https://doi.org/10.3390/min11040357.

Modi, P., J. C. Hower, R. K. Giri, et al. 2024. "Recovery of Rare Earth Elements From Coal Samples From the Sohagpur Coalfield, Madhya Pradesh, India." *International Journal of Coal Preparation and Utilization* 44: 219–239. https://doi.org/10.1080/19392699.2023.2179998.

Modi, P., A. Jamal, and N. Singh. 2022. "Coal Characterization and Occurrence of Rare Earth Elements in Coal and Coal-Ash of Sohagpur Coalfield, Madhya Pradesh, India." *International Journal of Coal Preparation and Utilization* 42: 2976–2989.

Mondal, D., S. Ghosh, P. Naveen, M. Kumar, A. Majumder, and A. Kumar Panda. 2021. "An Integrated Study on the Geochemical, Geophysical, and Geomechanical Characteristics of the Organic Deposits (Coal and CBM) of Eastern Sohagpur Coalfield, India." *Gondwana Research* 96: 122–141. https://doi.org/10.1016/j.gr.2021.03.016.

Mondal, D., P. Roy, and M. Kumar. 2020. "Monitoring the Strata Behavior in the Destressed Zone of a Shallow Indian Longwall Panel With Hard Sandstone Cover Using Mine-Microseismicity and Borehole

Televiewer Data." *Engineering Geology* 271: 105593. https://doi.org/10.1016/j.enggeo.2020.105593.

Mortazavi, M., R. Moussavi-Harami, A. Mahboubi, and M. Nadjafi. 2014. "Geochemistry of the Late Jurassic–Early Cretaceous Shales (Shurijeh Formation) in the Intracontinental Kopet-Dagh Basin, Northeastern Iran: Implication for Provenance, Source Weathering, and Paleoenvironments." *Arabian Journal of Geosciences* 7: 5353–5366. https://doi.org/10.1007/s12517-013-1081-4.

Mukhopadhyay, P. K. 1986. "Petrography of Selected Wilcox and Jockson Group Lignites From Tertiary of Texas." In *Geology of Gulf Coast Lignite*, edited by R. B. Finkelman, and D. J. Casagrande, 126–145. Annual Meeting in Geological Society of America, Coal Geology Division Field Trip.

Murthy, S., D. Agnihotri, D. Uhl, A. Jasper, and R. K. Singh. 2023. "Palaeoenvironmental and Stratigraphical Implications of the Palynoflora and Macro–Charcoal From the Early Permian of the Chuperbhita Coalfield, Rajmahal Basin, Jharkhand, India." *Journal of Palaeosciences* 72, no. 2: 141–151. https://doi.org/10.54991/jop.2023.1865.

Nandi, B. N., T. D. Brown, and G. K. Lee. 1977. "Inert Coal Macerals in Combustion." *Fuel* 56, no. 2: 125–130. https://doi.org/10.1016/0016-2361(77)90130-2.

Nath, M. 2021. "High Sulphur Paleogene Coals of North East India: Implications for Paleoenvironment and Paleoclimate." *Arabian Journal of Geosciences* 14: 1393. https://doi.org/10.1007/s12517-021-07703-1.

Navale, G. K. B., and R. S. Tiwari. 1967. "Petro-Palynological Study of Churcha Seam, Sohagpur Coalfield (MP), India." *Journal of the Geological Society of India* 8: 68–74. https://doi.org/10.17491/jgsi/1967/080112.

Painter, P. C., R. W. Snyder, M. Starsinic, M. M. Coleman, D. W. Kuehn, and A. Davis. 1981. "Concerning the Application of FT-IR to the Study of Coal: A Critical Assessment of Band Assignments and the Application of Spectral Analysis Programs." *Applied Spectroscopy* 35: 475–485. https://doi.org/10.1366/0003702814732256.

Painter, P., M. Starsinic, and M. Coleman. 1985. "Determination of Functional Groups in Coal by Fourier Transform Interferometry." In *Fourier Transform Infrared Spectra*, 169–241. Academic Press, Inc. https://doi.org/10.1016/B978-0-12-254104-9.50011-0.

Panda, M., S. M. Equeenuddin, and D. Mohanty. 2025. "Geochemical Characteristics of Talcher Coal, India: Insights on the Mode of Occurrence of Trace Elements and Palaeoenvironmental Conditions." *Geological Journal*. https://doi.org/10.1002/gj.5239.

Pareek, H. S. 1987. "Petrographic, Chemical, and Trace-Elemental Composition of the Coal of Sohagpur Coalfield, Madhya Pradesh, India." *International Journal of Coal Geology* 9: 187–207. https://doi.org/10.1016/0166-5162(87)90045-0.

Paul, A., S. Mukherjee, and M. Biswas. 2025. "Global Review on Shale: Focus on Hydrocarbon Geoscience & Carbon Sequestration." *Results in Earth Sciences* 3: 100088. https://doi.org/10.1016/j.rines.2025.100088.

Pazand, K. 2015. "Characterization of REE Geochemistry of Coals From the Sangrud Coal Mine, Alborz Coalfield, Iran." *Arabian Journal of Geosciences* 8: 8277–8282. https://doi.org/10.1007/s12517-015-1776-9.

Pickel, W., J. Kus, D. Flores, et al. 2017. "Classification of Liptinite—ICCP System 1994." *International Journal of Coal Geology* 169: 40–61. https://doi.org/10.1016/j.coal.2016.11.004.

Pillai, S. S. K., R. A. Sebastian, R. P. Mathews, et al. 2024. "Palaeodepositional Environment, Implications of Glossopteris Flora, and Organic Matter Characteristics From the Lower Permian, Karo Open Cast Mine, East Bokaro Coalfield, Damodar Basin, India." *Journal of Palaeogeography* 13, no. 3: 528–546. https://doi.org/10.1016/j.jop.2024.04.004.

Premlall, K., and L. Koech. 2025. "Influence of Coal Rank, Ash, Mineral Content, and Maceral Composition on CO2 Adsorption in South African Coals." *Cleaner Chemical Engineering* 11: 100160. https://doi.org/10.1016/j.clce.2025.100160.

Ram-Awatar, A. Mukhopadhyay, and S. Adhikari. 2004. "Palynostratigraphy of Sub-Surface Lower Gondwana, Pali Sediments, Sohagpur Coalfield, MP, India." *Journal of Palaeosciences* 53: 51–59. https://doi.org/10.54991/jop.2004.208.

Rathore, D., P. Gopinathan, P. K. Rajak, et al. 2025. "Elemental Composition and Petrographic Analysis of Coal in the Sohagpur Coalfield With Implications for Environmental Management." *Geological Journal*. https://doi.org/10.1002/gj.5185.

Roy, D. K., and B. P. Roser. 2013. "Climatic Control on the Composition of Carboniferous-Permian Gondwana Sediments, Khalaspir Basin, Bangladesh." *Gondwana Research* 23: 1163–1171. https://doi.org/10.1016/j.gr.2012.07.006.

Saikia, B. K., R. K. Boruah, and P. K. Gogoi. 2007. "XRD and FT-IR Investigations of Sub-Bituminous Assam Coals." *Bulletin of Materials Science* 30: 421–426. https://doi.org/10.1007/s12034-007-0068-8.

Shi, Q., J. Zhao, R. Ji, et al. 2024. "Depositional Environment and Origin of Inertinite-Rich Coal in the Ordos Basin." *Acta Geologica Sinica (English Edition)* 98, no. 4: 1064–1085. https://doi.org/10.1111/1755-6724.15180.

Singh, A. K. 2016a. "Petrographic and Geochemical Characterization of Coal From Talcher Coalfield, Mahanadi Basin, India." *Journal of the Geological Society of India* 87, no. 5: 525–534. https://doi.org/10.1007/s12594-016-0426-5.

Singh, A. K. 2016b. "Petrographic Characterization and Evolution of the Karharbari Coals, Talcher Coalfield, Orissa, India." *International Journal of Coal Science & Technology* 3: 133–147. https://doi.org/10.1007/s40789-016-0132-3.

Singh, A. K., A. Kumar, and J. K. Tripathi. 2019. "Mineralogical Characteristics of Low-Rank Coal From Nagaur, Rajasthan, India, and Their Implication for the Environment of Paleomire." *Energy Sources Part A Recovery Utilization and Environmental Effects* 43, no. 8: 893–904. https://doi.org/10.1080/15567036.2019.1632983.

Singh, A. K., and A. Kumar. 2019. "Assessment of Thermal Maturity, Source Rock Potential, and Paleodepositional Environment of the Paleogene Lignites in Barsingsar, Bikaner–Nagaur Basin, Western Rajasthan, India." *Natural Resources Research* 29, no. 2: 1283–1305. https://doi.org/10.1007/s11053-019-09502-8.

Singh, A. K., M. P. Singh, and P. K. Singh. 2015. "Microstructural Relation of Macerals With Mineral Matter in Eocene Coal." *Energy Sources, Part A: Recovery, Utilization and Environmental Effects* 37: 1089–1097. https://doi.org/10.1080/15567036.2011.603030.

Singh, A. K., P. K. Singh, M. P. Singh, and P. K. Banerjee. 2015. "Utilization of the Permian Coal Deposits of West Bokaro, India: A Petrochemical Evaluation." *Energy Sources, Part A: Recovery, Utilization and Environmental Effects* 37: 1081–1088. https://doi.org/10.1080/15567036.2011.603029.

Singh, B. D., and A. Singh. 2004. "Observations on Indian Permian Gondwana Coals Under Fluorescence Microscopy: An Overview." *Gondwana Research* 7: 143–151. https://doi.org/10.1016/S1342-937X(05)70313-0.

Singh, M. P., and A. K. Singh. 2000. "Petrographic Characteristics and Depositional Conditions of Eocene Coals of Platform Basins, Meghalaya, India." *International Journal of Coal Geology* 42: 315–356. https://doi.org/10.1016/S0166-5162(99)00045-2.

Singh, M. P., and P. K. Singh. 1996. "Petrographic Characterization and Evolution of the Permian Coal Deposits of the Rajmahal Basin, Bihar, India." *International Journal of Coal Geology* 29: 93–118. https://doi.org/10.1016/0166-5162(95)00005-4.

Singh, M. P., P. K. Singh, and A. K. Singh. 2003. "Petrography and Depositional Environments of the Permian Coal Deposits of Deoghar Basin, Bihar." *Journal of the Geological Society of India* 61, no. 4: 419–438.

Singh, P. K., M. P. Singh, A. K. Singh, and A. S. Naik. 2012. "Petrographic and Geochemical Characterization of Coals From Tiru Valley, Nagaland, NE India." *Energy Exploration & Exploitation* 30, no. 2: 171–191. https://doi.org/10.1260/0144-5987.30.2.171.

Srivastava, M. K., K. Kishor, M. Nath, and A. K. Singh. 2024. "Inorganic Geochemical Attributes of Jaintia Hills Coals, India: Implications for Paleo-Depositional Conditions." *Kuwait Journal of Science* 51: 100227. https://doi.org/10.1016/j.kjs.2024.100227.

Srivastava, M. K., K. Kishor, A. K. Singh, S. Mukherjee, and S. K. Bharti. 2025. "Tectonically Deformed Coal: Focus on Microstructures & Implications for Basin Evolution." *Marine and Petroleum Geology* 172: 107223. https://doi.org/10.1016/j.marpetgeo.2024.107223.

Suttner, L. J., and P. K. Dutta. 1986. "Alluvial Sandstone Composition and Paleoclimate, I. Framework Mineralogy." *SEPM Journal of Sedimentary Research* 56: 329–345. https://doi.org/10.1306/212F8909-2B24-11D7-8648000102C1865D.

Tchouatcha, M. S., A. P. Kouske, W. F. Galal, et al. 2023. "The Cretaceous of the Cameroon Atlantic Basin (Central Africa): Sediment Provenance, Correlation, Paleoenvironment, and Paleogeographic Evolution of the Eastern Proto-Atlantic Margin (Central Gondwana)." *Environment and Earth Science* 82: 103. https://doi.org/10.1007/s12665-023-10765-x.

Teichmuller, M., and M. Wolf. 1977. "Application of Fluorescence Microscopy in Coal Petrology and Oil Exploration." *Journal of Microscopy* 109: 49–73. https://doi.org/10.1111/j.1365-2818.1977.tb01116.x.

Wahengbam, A., Y. R. Singh, L. S. Singh, and C. K. Singh. 2025. "Source Rock and Palaeoecology of the Permian Damuda Formation, Group, Sikkim: Rock–Eval Pyrolysis and Organic Matter Approach." *Journal of Earth System Science* 134: 62. https://doi.org/10.1007/s12040-025-02521-5.

Wang, W., Y. Qin, D. Song, and X. Fu. 2003. "REE Geochemistry of Moderate- and High-Sulfur Coals From North Shanxi, China." *Chinese Journal of Geochemistry* 22: 123–132. https://doi.org/10.1007/bf02831521.

Ward, C. R. 2002. "Analysis and Significance of Mineral Matter in Coal Seams." *International Journal of Coal Geology* 50: 135–168. https://doi.org/10.1016/S0166-5162(02)00117-9.